An experimental study on Rosensweig instability of a ferrofluid droplet

Ching-Yao Chen and Z.-Y. Cheng

Citation: Physics of Fluids (1994-present) **20**, 054105 (2008); doi: 10.1063/1.2929372
View online: http://dx.doi.org/10.1063/1.2929372
View Table of Contents: http://scitation.aip.org/content/aip/journal/pof2/20/5?ver=pdfcov
Published by the AIP Publishing

An experimental study on Rosensweig instability of a ferrofluid droplet

Ching-Yao Chen[1,a)] and Z.-Y. Cheng[2]
[1]*Department of Mechanical Engineering, National Chiao Tung University, Hsinchu 300, Taiwan, Republic of China*
[2]*Department of Mechanical Engineering, National Yunlin University of Science and Technology, Yunlin 640, Taiwan, Republic of China*

(Received 8 October 2007; accepted 9 April 2008; published online 30 May 2008)

We experimentally investigate the interfacial morphologies of Rosensweig instability on an extremely thin layer of ferrofluid droplets under a constant perpendicular magnetic field. Striking patterns consisting of numerous subscale droplets that developed from Rosensweig instability are observed. For a dry plate, on which surface tension dominates, the breaking pattern of subscale droplets can be characterized by a dimensionless magnetic Bond number Bo_m. In general, a more pronounced instability, which is evident by a greater number of breaking subscale droplets N, arises with a higher Bo_m. For a magnetic Bond number that is larger than a critical value, we identify a new mode of interfacial breakup pattern, where the central droplet is torn apart with major mass loss. In addition, we found that the volume fractions of breaking subscale droplets are strongly affected by the height variation of the initial fluid surface and appear unevenly distributed with dominance of a central droplet. On the other hand, for a prewetted plate, a nearly flat fluid surface is achieved due to a smaller contact angle, which then leads to virtually evenly distributed subscale droplets. A global size for all breaking subscale droplets is observed regardless of their initial diameters. The number of breaking subscale droplets (N) and the diameter of the initial droplet (D) can be approximated by a quadratic proportionality of $N \sim D^2$. © *2008 American Institute of Physics*.
[DOI: 10.1063/1.2929372]

I. INTRODUCTION AND EXPERIMENTAL SETUP

Ferrofluids consist of layers of surfactants coated on nanomagnetic particles to form colloidal suspensions in carrier fluids, such as water and oil. Manipulated by an external magnetic field, magnetic fluids have been widely used in engineering applications.[1,2] In particular, interfacial instability on the free surface of a horizontal magnetic layer, which is referred to as Rosensweig instability as it was first studied by Cowley and Rosensweig,[3] also interests researchers from both scientific and practical points of views. When the magnetic strength reaches a critical value, a sudden transition from an original flat surface to a hexagonal pattern of three-dimensional liquid crests, or the so-called Rosensweig crests, occurs. These Rosensweig crest patterns are experimentally demonstrated by means of radioscopy.[4] In addition, an interesting rupture in continuity of an extremely thin film with individual droplets that preserve the hexagonal geometry is reported.[5] Moreover, the dynamics of the crests have also been intensively studied both experimentally[6–9] and theoretically.[10–12] However, these researches focus mainly on the magnetic fluid layer at a relatively larger scale. With advances in microtechnology, it is interesting to further investigate the instability phenomena of an extremely thin film, in which stronger effects by surface tension might lead to new interesting phenomena.

Recently, Rosensweig instability of a thin film of ferrofluid droplets with diameters ranging from $O(10^2-10^3)$ μm under an instantaneous perpendicular magnetic field on a dry plate was investigated.[13–15] The ferrodroplet is observed to break up into numerous subscale droplets with the breakup pattern dependent on its initial diameter and field conditions. This particularly simple phenomenon of droplet rupture can possibly be applied as a noninvasive means for the partition of microscale droplets. Four modes of striking film rupture instabilities are reported.[13,14] Mode I instability shows a fully evolved subscale droplet, which is referred to as the *central droplet*, along with a separated outer fluid annulus. If the size of the initial droplet is increased past a certain threshold, the outer annulus is further destabilized and fully evolves into mode II instability, which forms an additional outer circular array of subscale droplets, denoted as *subdroplets*. A more vigorous mode III instability is observed for an even bigger initial droplet, in which additional secondary subscale droplets are generated in the middle region and within the intervals of subdroplets in the outer array, which are referred to as *middle subdroplets* and *derivative subdroplets*, respectively. If the size of the droplet is further increased, a complex mode IV pattern is formed in which a more disorderly arrangement with a multiarray of additional middle subdroplets in the middle region and numerous derivative subdroplets within the outer array. Complete topologies of the four ruptured modes can be found in Refs. 13 and 14 as well as in the figures presented later in the current study. Nevertheless, only the top views of the breakup topologies are investigated in prior research, in which the very important third dimensional effects of Rosensweig crests are not included for analysis. As a result, the mechanisms acting on the ferroflu-

a)Author to whom correspondence should be addressed. Electronic mail: chingyao@mail.nctu.edu.tw.

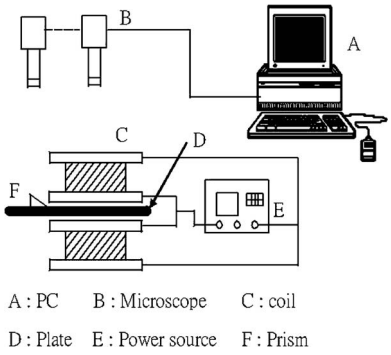

FIG. 1. Principle sketch of experimental setup: The experimental setup consists of an extremely thin layer of ferrofluid droplets placed on a glass plate subjected to a perpendicular field. The field strength is produced by a pair of coils in the Helmholtz configuration powered by a computerized programmable power source. The top and side (via reflection of a prism) views are recorded by CCD cameras.

ids cannot be fully understood and analyzed. Therefore, important issues, such as the number and volume of the breaking subscale droplets, which are important for practical applications, need to be addressed. In the present investigation, both the top and side views are recorded to give more comprehensive explanations for the film rupture mechanism in terms of general dimensionless parameters. Furthermore, similar experiments are carried out for situations in prewetted conditions to resolve the uneven formation of breaking subscale droplets on a dry plate.

The experimental setup consists of a circular thin layer of a ferrodroplet placed on a glass plate subjected to a perpendicular magnetic field as the principle sketch shown in Fig. 1. A light mineral oil-based ferrofluid (EMG901) produced by Ferrotec Corporation is used in the experiments. The saturation magnetization (M_s), density (ρ), and fluid/air surface tension (γ) of this particular ferrofluid are $M_s = 600$ G, $\rho = 1530$ kg/m^3, and $\gamma = 25$ mN/m, respectively. The field strength is generated by a pair of coils in the Helmholtz configuration. The power source is turned on instantaneously to generate a uniform field strength of $H = 743$ Oe and kept constant by fixing the current intensity. We record the interfacial morphologies of the ferrodroplet using charge-coupled device (CCD) cameras. Side views are taken via reflections from a prism.

II. RESULTS AND DISCUSSION

A. Experiments on a dry plate

We first describe the observation of a representative case for a ferrodroplet with an initial diameter of $D \approx 900$ μm (measured from the top view), as shown in Fig. 2. The top and side views of the initial state are shown in Figs. 2(a) and 2(b), respectively. Because of reflection, only the right half (slightly darker) part of the side view image shown in Fig. 2(b) represents the actual image of the ferrodroplet. The initial side view appears as a typical hydrophilic thin layer with a maximum central height h_0 estimated to be approximately 54 μm. When a perpendicular magnetic field is present, the magnetized ferrodroplet is subjected to an instant third dimensional upward force. This upward force lifts the droplet and, consequently, pulls the circumference toward the center. However, surface tension resists this sudden pulling effect. As a result, the drop is broken up into numerous subscale droplets, and the top and side views at the final equilibrium state are shown in Figs. 2(c) and 2(d), respectively. Consistent with findings reported in Refs. 13–15, mode II instability is reproduced, as shown in Fig. 2(c), which includes the largest central droplet with a circular array of smaller and nearly evenly distributed subdroplets surrounding it. For this case,

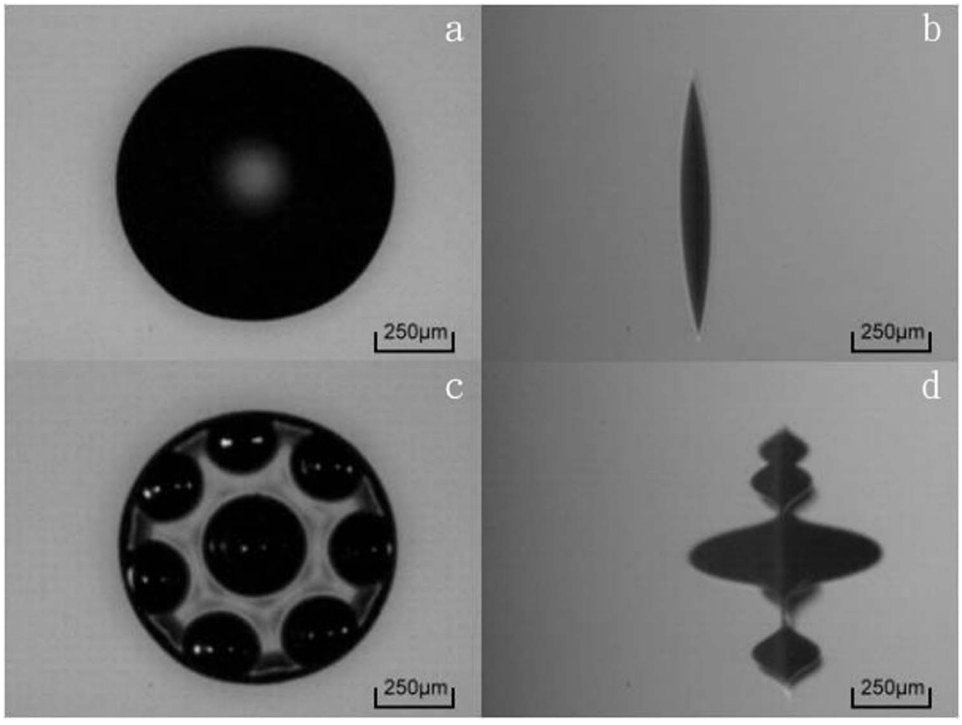

FIG. 2. Snapshots of a droplet with an initial diameter of $D \approx 900$ μm under a field strength of $H = 743$ Oe ($\mathrm{Bo}_m = 92$) for the representative case: (a) top view and (b) side view under zero field strength, and (c) top view and (d) side view in the final equilibrium state. The gravitational force is toward the left in the side views (b) and (d). Because of reflection, only the right half (slightly darker) part of side view images represents the actual shape of the ferrofluid surface. Mode II instability, which consists of a dominant central droplet with an outer circular array of seven subdroplets, is observed in the presence of a magnetic field.

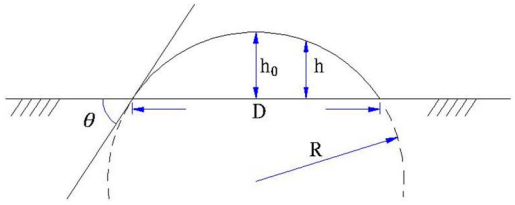

FIG. 3. (Color online) Schematic of a spherical cap.

eight breaking subscale droplets are observed in total ($N=8$). This particular number of breaking subscale droplets can be used to quantitatively determine the prominence of breakup instability. More detailed transient morphological evolutions of the top view are referred to Ref. 13. The subscale droplets observed from the top views are not plain two-dimensional circular films but rather typical three-dimensional Rosensweig crests with sharp spikes, as shown by the side views in Fig. 2(d). These three-dimensional structures explain the decrease in the total area occupied by ferrofluids. Nevertheless, in order to be consistent with the top circular morphologies, we simply refer to them as droplets. The corresponding side view of the ruptured droplet [Fig. 2(d)] clearly demonstrates domination of the central droplet (the highest central Rosensweig crest) over those outer subdroplets (or outer lower Rosensweig crests). The height of the central droplet is much larger than that of the subdroplets, whose heights are nearly identical.

In order to analyze the rupture instability in a more quantitative way, the mechanisms acting on the ferrodroplet need to be clarified. The initial shape of the ferrofluid layer, as shown in Fig. 2(b), is determined by the balance of the opposing forces of the hydrostatic pressure ρgR caused by gravity and the Laplace pressure γ/R due to surface tension, where R denotes the radius of curvature. By applying the physical properties of ferrofluids, a capillary radius $R_c=\sqrt{\gamma/\rho g}\approx 14$ mm can be obtained if the two pressures are balanced. When $R \ll R_c$, the Laplace pressure dominates, and the initial shape of the fluid surface tends to be a spherical cap. The scales of the ferrodroplets investigated in the present study fully satisfy this condition, so the initial shape of the side view can be properly represented by a spherical cap, as the schematic in Fig. 3 demonstrates. On the other hand, the final equilibrium state of the rupture instability is dominated primarily by the upward lifting magnetic force and the local constraint of surface tension so that a dimensionless parameter of magnetic Bond number can be defined. We would like to point out that the surface deformation is induced by a magnetic field that is perpendicular to the plate. As a result, the actual constraints of surface tension are determined by the local curvatures perpendicular to the plate, which vary depending on the location with a maximum value of R occurring at the center. This characteristic value is used for the global magnetic Bond number as $\mathrm{Bo}_m=\mu_0 MHR/2\gamma$ to describe the pattern formation. It is expected that a higher magnetic Bond number would lead to a more vigorous breakup instability, which can be represented by the formation of a higher number of subscale droplets. By geometrical formulation, the characteristic quantities of interests, i.e., the contact angle (θ) and radius of curvature (R), are obtained as $R=1.9$ mm and $\theta=13.7°$, respectively. At the present representative case, the radius of curvature associated with correspondent field condition and fluid properties yield a magnetic Bond number $\mathrm{Bo}_m=92$ and results in a breakup pattern of eight subscale droplets ($N=8$).

Another interesting quantity worth discussing is the characteristic volume fraction of each individual breaking subscale droplet, which is defined by the volume ratio of the subscale droplet to the original spherical cap (V_{cap}). The exact volume of the spherical cap can be obtained by geometrical formulation as $V_{\mathrm{cap}}=17.3$ nl, correspondingly, at the present condition. We approximate the volume of each subscale droplet, both the central droplet and outlying subdroplets, as circular cones. Consequently, the volume fractions of the central droplet (V_c) and the subdroplet (V_s) can be compared to determine the dominance of the central droplet. In the present representative case, the dominance of central droplet ($V_c=0.375$, $V_s=0.06$) is clearly demonstrated and is attributed to the variation in initial height along the substrate plate, denoted as h, as depicted in Fig. 3. Based on the reason that was partially presented in the previous paragraph, the formation of breaking subscale droplets is determined primarily by the competition of magnetic energy and local surface constraints. However, surface deformation is perpendicular rather than radial to the substrate plate along the field direction. Therefore, surface tension constraints are affected by the local radii of the curvature perpendicular to the plate which vary spatially and can be represented by the local height h. Although magnetic force is uniformly distributed, the predominance of the central height (h_0) naturally leads to the smallest local vertical curvature and, consequently, the weakest surface constraint. On the other hand, larger curvatures result from lower surface heights near the contact region. As a result, the weaker constraint of surface tension near the center allows for a major surface deformation, and hence, the formation of a dominant central droplet. We would like to point out that the dominance of a central droplet is a disadvantage if a uniform breakup of subscale droplets is desired for certain applications.

Next, we investigate the ferrodroplets under different initial conditions. In general, a smaller droplet leads to a lower magnetic Bond number. For a smaller magnetic Bond number ($D\approx 800$ μm, $\mathrm{Bo}_m=44$), the breakup of ferrodroplet shows a different pattern of mode I instability,[13,14] as shown by the top and side views in the equilibrium state in Figs. 4(a) and 4(b), respectively. While the formation of the central droplet is still similar to the previous representative case ($\mathrm{Bo}_m=92$), a fluid annulus, instead of a circular array of subdroplets, is observed around the central droplet. This formation of a single central droplet ($N=1$) indicates a more stable situation for a smaller magnetic Bond number, as expected. Shown in Figs. 4(c) and 4(d) is the breaking pattern for a higher magnetic Bond number ($\mathrm{Bo}_m=74.5$) which appears to be similar to a mode II instability as with the representative case. On the other hand, if the magnetic Bond number is increased to 93, which is slightly higher than the representative case, breakup instability is turned into mode III instability, as shown in Figs. 4(e) and 4(f). Besides the previously

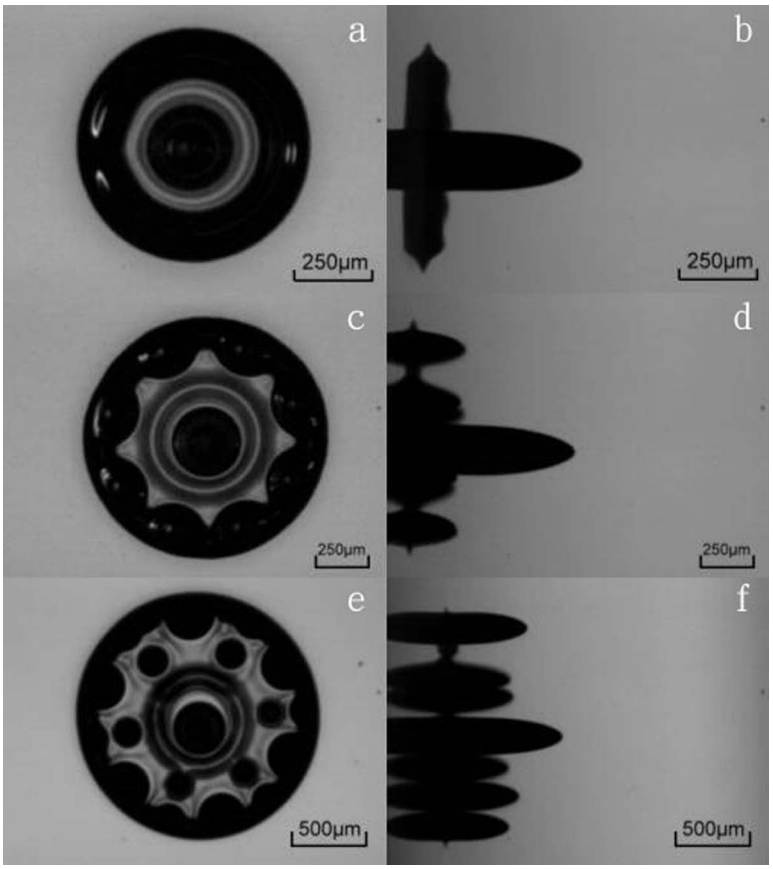

FIG. 4. Top row: (a) top view and (b) side view. Mode I instability for the case with $Bo_m=44$: the drop is ruptured into a central droplet surrounded by a fluid annulus. Middle row: (c) top view and (d) side view of a mode II instability with $Bo_m=74.5$. Bottom row: (e) top view and (f) side view for the case with $Bo_m=93$: a more vigorous mode III instability with an additional circular array of middle subdroplets in the middle region and smaller derivative subdroplets within the intervals of outer subdroplets is observed.

observed central droplet with many subdroplets in the outer circular array, an additional circular array of middle subdroplets is formed in the middle region. Furthermore, smaller derivative subdroplets appear at the intervals of subdroplets in the outer array. The number of distinguishable breaking subscale droplets is increased to $N=19$. For even higher magnetic Bond numbers ($131 \leqslant Bo_m \leqslant 143$), extremely vigorous breakups of mode IV instability are observed. For droplets with a magnetic Bond number greater than 149, even the topology of the top view at final equilibrium state still retains the main features of mode IV instability. An example with $Bo_m=149$ is shown in Fig. 5(c), where a very large volume of the central droplet is vertically pinched off and pulled apart from the plate. The sequential snapshots of the pinch off are shown in Figs. 5(a) and 5(b) and show a significant mass loss of the central droplet after vertical pinch off. This vertical pinch off is a result of the further weakening of the local surface tension at the central region which is unable to sustain the magnetic upward lift force. We would like to point out that this major mass loss of the central droplet is undesirable for applications. As a result, the applicability of the current method for generating subscale droplets is limited by the maximum magnetic Bond number. We refer to this mass loss of central droplet as the new mode V instability.

We summarize the results by plotting the number of all distinguishable subscale droplets (N) and the volume fractions of the central droplet (V_c) and subdroplets (V_s) at various magnetic Bond numbers (Bo_m), as shown in Figs. 6 and 7, respectively. Apparent sudden jumps, which indicate mode changes, are clearly observed in Fig. 6. Consistent with early studies,[13,14] four major ranges ($Bo_m \leqslant 44$, $57 \leqslant Bo_m \leqslant 92$, $93 \leqslant Bo_m \leqslant 126$, and $Bo_m \geqslant 131$) that correspond to mode I–IV instabilities can be identified. However, we would like to point out again that the new mode V instability, which is associated with significant mass loss of the central droplet, occurs for $Bo_m \geqslant 149$, even though the quantitative trend remains similar to the mode IV instability. In general, the number of subscale droplets increases with the magnetic Bond

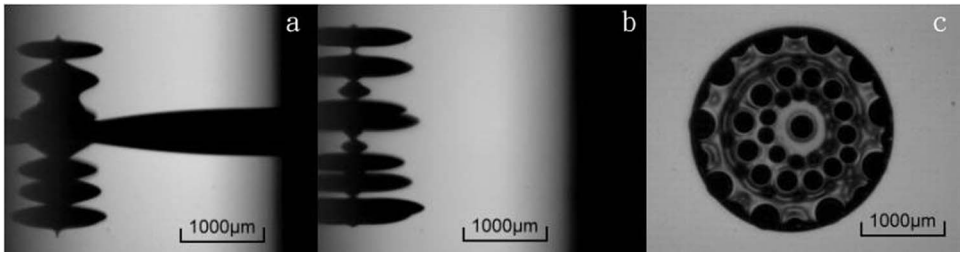

FIG. 5. Snapshots for the case with $Bo_m=149$: even the top view (c) for the final equilibrium state maintains the features of mode IV instability, the side views images clearly demonstrate pinched off (a) and pulled away (b) of the central droplet. This new phenomenon of mass loss from the central droplet is categorized as mode V instability.

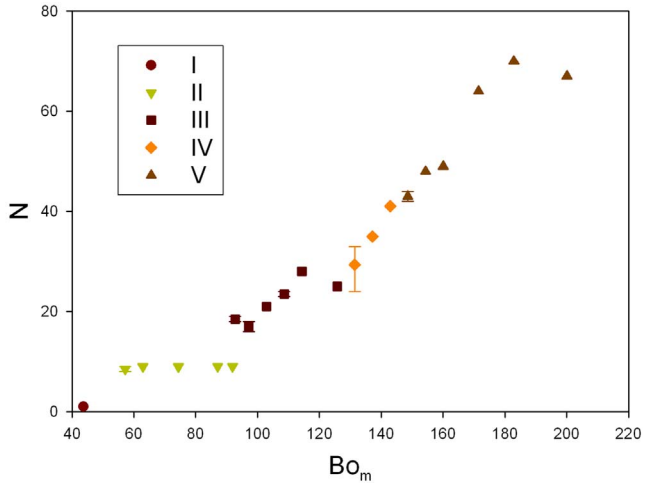

FIG. 6. (Color online) Number of breaking subscale droplets (N) vs the magnetic Bond number (Bo_m) for the case of a dry plate. The plot clearly shows sudden jumps near critical magnetic Bond number that lead to different modes of rupture patterns. In general, the number of subscale droplets increases with the higher values of magnetic Bond number.

number. No particular numerical correlations are found to describe the dependence between them. However, the volume fractions of subscale droplets shown in Fig. 7 do not follow such similar monotonic trend, as can bee seen from Fig. 7. While the volume fractions of subdroplets V_s depend weakly on the magnetic Bond number Bo_m, the volume fractions of the central droplet fluctuate significantly. These different trends can be understood by the variation of the local constraints. As explained previously, the local constraint is directly related to the corresponding vertical height (h). The outer subdroplets are strongly affected by the local heights in the contact region which are greatly influenced by contact angles. As a result, the variation in local surface constraints

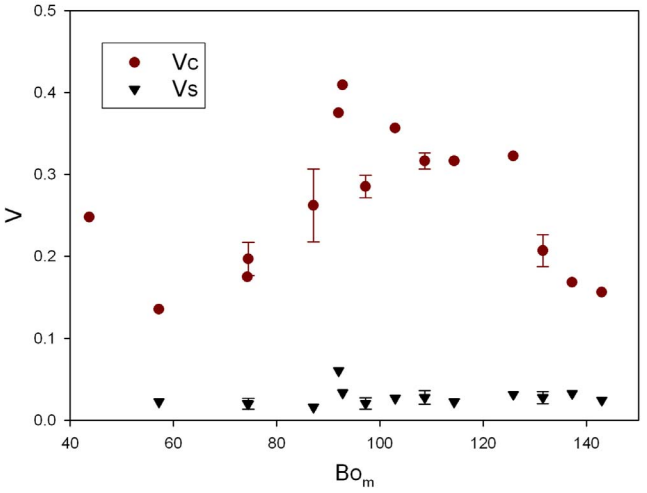

FIG. 7. (Color online) Volume factions of each individual subscale droplet vs the magnetic Bond number (Bo_m) for the case of a dry plate. While the volume fractions of subdroplets (V_s) depend weakly on the magnetic Bond numbers, volume fractions of the central droplet (V_c) vary significantly because of the evolution of different modes of instability. Significant volume dominance of the central droplet is clearly observed compared to the subdroplets.

would not be too significant under the same surface condition. Consequently, the volume factions V_s vary insignificantly. On the other hand, the volume of the central droplet is determined by two factors, i.e., the local surface constraint in the central region (Bo_m) and the number of breaking subscale droplets (N). In general, if N remains basically unchanged, which corresponds to the same breaking pattern, the volume of central droplet would be greater for a weaker local constraint (or a larger Bo_m). However, once more breaking subscale droplets are formed, either because of a mode change or simply through the generation of more middle subdroplets by continuously increasing Bo_m, to share the fluid volume, V_c would be reduced. This explains the dramatic volume variation of the central droplet as Bo_m varies. As shown in Fig. 7, three significant drops in V_c are observed at $\mathrm{Bo}_m = 57$, 97, and 131, where the mode transitions occur. In addition, within the range of mode II instability ($57 \leqslant \mathrm{Bo}_m \leqslant 92$), where N remains nearly unchanged, V_c increases for a higher value of Bo_m, which can be attributed to a weaker local surface constraint. As for the regions of modes III and IV, although the surface constraints weaken for higher values of Bo_m, the formation of additional middle subdroplets suppresses the growth of V_c, resulting in a gradual volume reduction in V_c. Nevertheless, the dominance of the central droplet over the subdroplets is always preserved.

B. Results on a prewetted plate

Based on the results from a dry plate discussed above, it can be concluded that the vertical curvature (or local height h) of the fluid surface is crucial in determining the pattern of instability. The variation in vertical curvature leads to disadvantages for potential applications of microdroplet partitions, namely the dominance of central droplet through mode I–IV instabilities or major mass loss of central droplet occurring in the mode V regime. An obvious solution to these problems is to produce a flatter initial surface profile so that the local constraints of surface tension are more uniformly distributed. Consequently, modifying the wetting conditions on the plate, which would lead to a different contact angle, is a natural means to manipulate the patterns of instability. In this section, we present similar experiments on a plate that is prewetted with mineral oil. A corresponding case of $D \approx 900$ μm, which can be compared directly to the representative case in Fig. 2, is shown in Fig. 8. The change in contact surface immediately reduces the contact angle dramatically as the side view at initial state shows in Fig. 8(b). The radius of curvature R for the corresponding fluid film is therefore compatible to the capillary radius R_c. As a result, both surface tension and gravity play significant roles in determining the initial shape of the fluid surface. A nearly flat fluid surface of extremely thin film is formed on the present prewetted surface as compared to a nearly spherical cap on the previous dry plate. Since it is difficult to accurately measure the puddle thickness of fluid film to obtain the contact angle and radius of curvature for the prewetted plate case, dimensional parameters, such as the initial diameters and field strengths, are used instead of the global parameter Bo_m.

The extremely thin and nearly flat surface leads to a

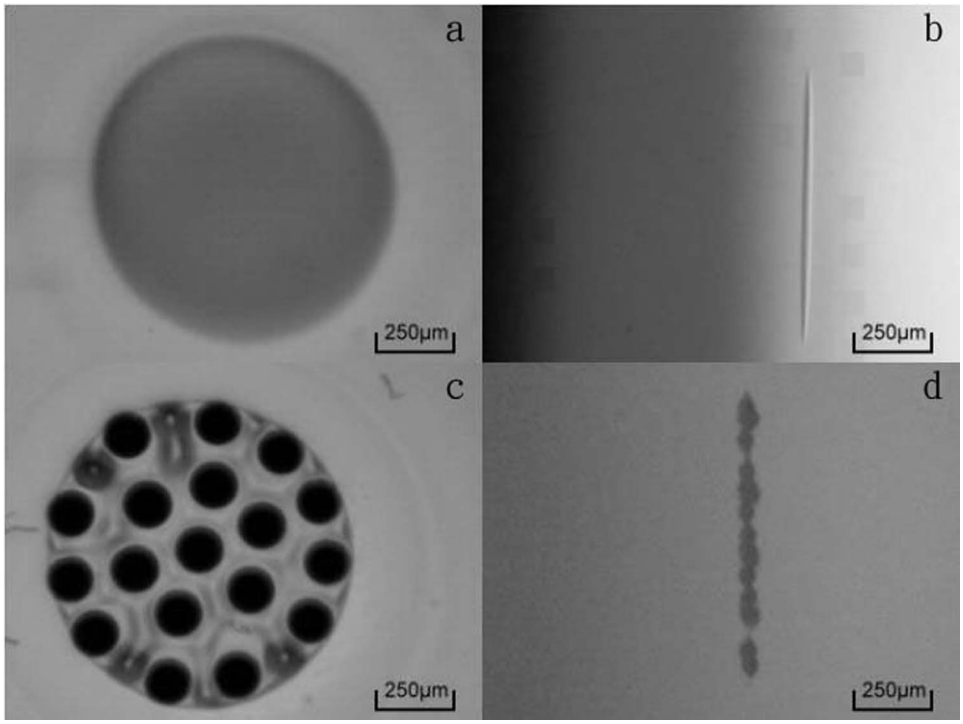

FIG. 8. A droplet of $D \approx 900$ μm on a prewetted plate: (a) top view and (b) side view under zero field strength, and (c) top view and (d) side view in the final equilibrium state. A nearly flat surface results in more breaking subscale droplets. Furthermore, the dominance of the central droplet is no longer observed with each subscale droplet appearing nearly a unique size and height.

nearly uniform and very weak constraint of surface tension along the interface, so that a greater number of breaking subscale droplets ($N=19$) is generated at the presence of the magnetic field, as shown in Figs. 8(c) and 8(d). The dominance of the central droplet is no longer observed with all the subscale droplets appearing with a unique size and height. It is noteworthy to compare the present experiments to a very relevant theoretical study by Blums *et al.*[2] By applying the method of simulated annealing, the equilibrium configurations of magnetic dipoles are theoretically obtained. An almost identical topology by theoretical prediction (see Fig. 2.74 in Ref. 2) to the present case is reported. Under the present prewetted condition, in which the droplet is equally divided, the amazing agreement indicates that the interactions between the subscale droplets mimic those of magnetic dipoles. As a result, the configuration, which includes the topology and the number of subscale droplets, can be studied and even possibly further predicted by a sophisticated theoretical model.

The pattern of a nearly uniform breakup is nicely preserved for various initial sizes, such as $D=1400$, 1600, 2300, and 3300 μm, as shown in Figs. 9(a)–9(d), respectively. Based on observations of all the experimented sizes ($D \leqslant 3300$ μm), we found that, as expected, a larger droplet generates a larger number of subscale droplets. In addition, all of the individual subscale droplets remain quite close in size by visual inspection, regardless of the initial diameters. The plot of N and D, shown in Fig. 10, appears to be a smooth curve without sudden jumps. The curve follows a correlation of a near quadratic proportionality of $N \sim D^2$ approximately. Under the situation of a constant height for all individual subdroplets, the approximation of quadratic proportionality provides a further quantitative confirmation of a global size for all breaking subscale droplets regardless their initial diameters.

III. CONCLUSION

Experiments are presented to investigate the interfacial morphologies of an extremely thin layer of ferrofluid under a constant perpendicular magnetic field. Vigorous breakups of the initial droplet into numerous subscale droplets are demonstrated. This particularly simple phenomenon of droplet breakups can possibly be applied as a noninvasive means for the partition of microscale droplets. Two important issues that are relevant to the applications, i.e., the number of breaking subscale droplets and their volumes, are addressed. On a dry plate, where the surface tension dominates, the initial profile of the fluid surface can be properly represented by a spherical cap. A global dimensionless magnetic Bond number (Bo_m) can be defined to describe the breakup pattern formation. We have shown a strong dependence of the breakup patterns on the magnetic Bond number. Consistent with previous studies,[13,14] four modes of ruptured instability are identified, including three well-ordered patterns for magnetic Bond numbers ranging from $44 \leqslant \mathrm{Bo}_m \leqslant 126$ and a more complex and disorder mode IV instability for a higher magnetic Bond number of $\mathrm{Bo}_m \geqslant 131$. In addition, a new mode V instability, which has a top view topology that remains similar to that of mode IV instability, occurs for an even higher magnetic Bond number of $\mathrm{Bo}_m \geqslant 149$, except that the central droplet is pulled apart. In general, a larger number of subscale droplets results from a higher magnetic Bond number. No particular numerical correlations are found to describe the dependence between the number of subscale

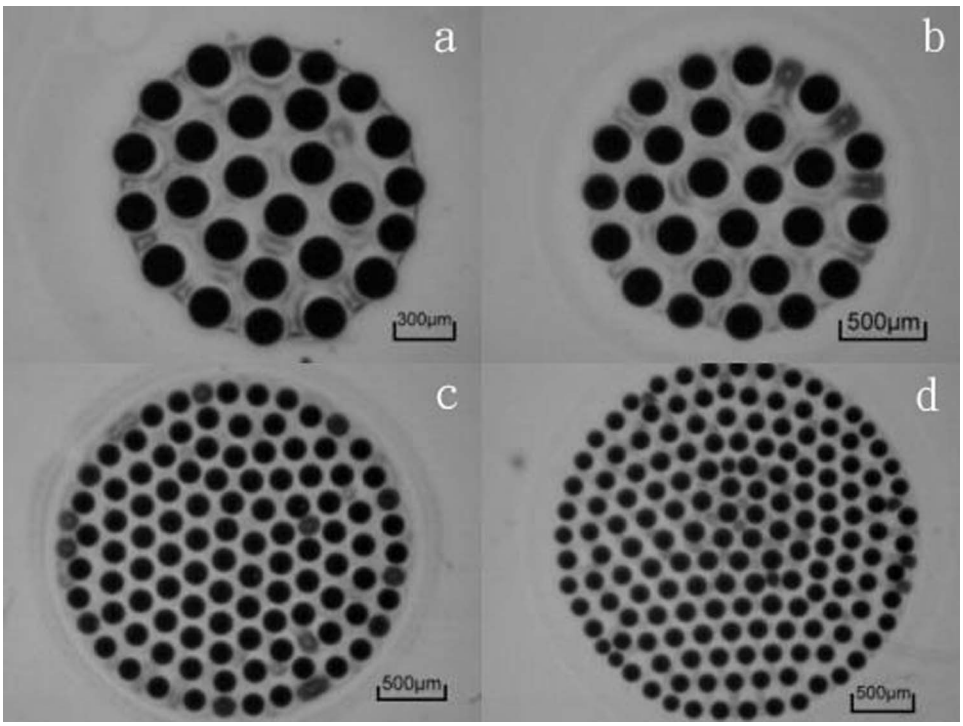

FIG. 9. Patterns of nearly uniform breakup on a prewetted plate are nicely preserved for various initial sizes of (a) $D \approx 1400\ \mu$m, (b) $D \approx 1600\ \mu$m, (c) $D \approx 2300\ \mu$m, and (d) $D \approx 3300\ \mu$m. By visual inspection, the size of the subscale droplets appears to be the same, even among different initial diameters.

droplets and the magnetic Bond number. On the other hand, because of significant height variation along the ferrofluid surface, domination of the central droplet is always observed through the ranges of mode I–IV instabilities. The volume of the central droplet is determined by two factors, i.e., the local constraints of surface tension and the number of breaking subscale droplets. In general, if N remains closely under the same breaking pattern in the regime of mode II instability, the volume fraction of central droplet would be greater for weaker local constrain (or a larger magnetic Bond number). However, once more breaking subscale droplets are formed to share the fluid volume, either because of the mode change or simply the generation of more middle subdroplets by the continuous increase in the magnetic Bond number, the volume fraction of the central droplet is reduced. The uneven breakup of subscale droplets through the regimes of mode I–IV instability, as well as the significant mass loss that occurs in mode V region, are disadvantages if a uniform partition of droplets for further application is desired. These disadvantages can be resolved by prewetting the plate.

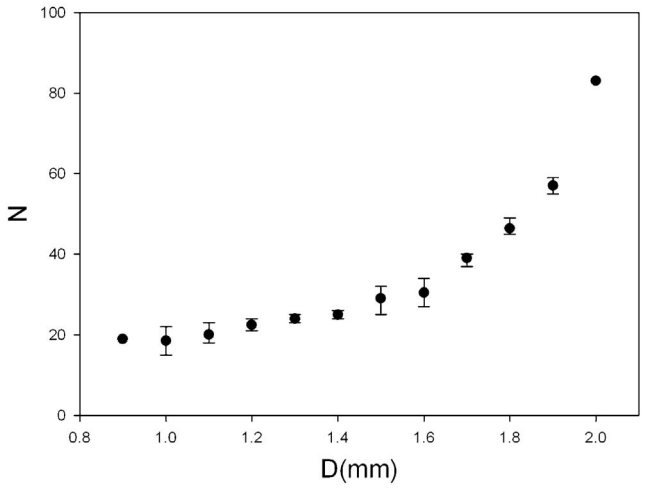

FIG. 10. Numbers of breaking subscale droplets N vs initial droplet diameters D on a prewetted plate: the correlation can be approximated by a quadratic proportionality of $N \sim D^2$. No dramatic mode transition occurs for any of the cases on a prewetted plate.

A plate prewetted with mineral oil reduces the contact angle dramatically and leads to a nearly flat fluid surface without significant height variation in the initial state. It results in a nearly uniform local surface tension, so that the volumes of all breaking subscale droplets are basically equal. Furthermore, the topology is almost identical to the simulated equilibrium configuration of magnetic dipoles.[2] The excellent agreement suggests that interactions between subscale droplets mimic those of magnetic dipoles. In addition, the size of each breaking subscale droplet is weakly dependent on the initial diameters of the ferrodroplet. The number of breaking subscale droplets (N) and the diameter of initial droplet (D) can be approximated by a quadratic proportionality of $N \sim D2$, which provides further support of a global size for all breaking subscale droplets regardless their initial diameters.

ACKNOWLEDGMENTS

C.-Y. Chen thanks the National Science Council of the Republic of China for financial support of this research under Grant No. NSC 95-2221-E-009-369-MY3.

[1] R. Rosensweig, *Ferrohydrodynamics* (Cambridge University Press, New York, 1985).
[2] E. Blums, A. Cebers, and M. M. Maiorov, *Magnetic Fluids* (Walter de Gruyter, Berlin, 1997).
[3] M. D. Cowley and R. E. Rosensweig, "The interfacial stability of a ferromagnetic fluid," J. Fluid Mech. **30**, 671 (1967).

[4]R. Richter and J. Blasing, "Measuring surface deformations in magnetic fluids by radioscopy," Rev. Sci. Instrum. **72**, 1729 (2001).
[5]B. M. Berkovsky and V. Bashtovoi, "Instabilities of magnetic fluids leading to a rupture of continuity," IEEE Trans. Magn. **MAG-16**, 288 (1980).
[6]F. Elias, C. Flament, and J.-C. Bacri, "Motion of an asymmetric ferrofluid drop under a homogeneous time-dependent magnetic field," Phys. Rev. Lett. **77**, 643 (1996).
[7]R. Rosensweig, S. Elborai, S.-H. Lee, and M. Zahn, "Ferrofluid meniscus in a horizontal or vertical magnetic field," J. Magn. Magn. Mater. **289**, 192 (2005).
[8]M. Zahn, "Magnetic fluids and nanoparticle applications to nanotechnology," J. Nanopart. Res. **3**, 73 (2001).
[9]R. Richter and I. V. Barashenkov, "Two-dimensional solitons on the surface of magnetic fluids," Phys. Rev. Lett. **94**, 184503 (2005).
[10]O. Sero-Guillaume, D. Zouaoui, D. Bernardin, and J. Brancher, "The shape of a magnetic liquid drop," J. Fluid Mech. **241**, 215 (1992).
[11]A. Lange, H. Langer, and A. Engel, "Dynamics of a single peak of the Rosensweig instability in a magnetic fluid," Physica D **140**, 294 (2000).
[12]S. Bohlius, H. Pleiner, and H. Brand, "Solution of the adjoint problem for instability with a deformable surface: Rosensweig and Marangoni instability," Phys. Fluids **19**, 094103 (2007).
[13]C.-Y. Chen and L.-W. Lo, "Breakup of thin films of micro magnetic drops in perpendicular fields," J. Magn. Magn. Mater. **305**, 440 (2006).
[14]C.-Y. Chen and L.-W. Lo, "Influences of field conditions to the rupturing instability of a circular magnetic thin film," Magnetohydrodynamics **42**, 31 (2006).
[15]C.-Y. Chen, C.-H. Chen, and L.-W. Lo, "Breakup and separation of micro magnetic droplets in a perpendicular field," J. Magn. Magn. Mater. **310**, 2832 (2007).